Astronomy & Astrophysics manuscript no. aa
July 24, 2024

Revisiting Empirical Solar Energetic Particle Scaling Relations

II. Coronal Mass Ejections

Athanasios Papaioannou[1], Konstantin Herbst[2], Tobias Ramm[3], David Lario[4], and Astrid M. Veronig[5]

[1] Institute for Astronomy, Astrophysics, Space Applications and Remote Sensing (IAASARS), National Observatory of Athens, I. Metaxa & Vas. Pavlou St., 15236 Penteli, Greece
e-mail: atpapaio@astro.noa.gr
[2] Institut für Experimentelle und Angewandte Physik, Christian-Albrechts-Universität zu Kiel, 24118 Kiel, Germany
[3] Institut für Theoretische Physik und Astrophysik, Christian-Albrechts-Universität zu Kiel, 24118 Kiel, Germany
[4] NASA, Goddard Space Flight Center, Heliophysics Science Division, Greenbelt, MD 20771, USA
[5] Institute of Physics & Kanzelhöhe Observatory for Solar and Environmental Research, University of Graz, A-8010 Graz, Austria

July 24, 2024

ABSTRACT

Aims. The space radiation environment conditions and the maximum expected coronal mass ejection (CME) speed are being assessed through the investigation of scaling laws between the peak proton flux and fluence of Solar Energetic Particle (SEP) events with the speed of the CMEs.
Methods. We utilize a complete catalog of SEP events, covering the last ~25 years of CME observations (i.e. 1997 to 2017). We calculate the peak proton fluxes and integrated event fluences for those events reaching an integral energy of up to E> 100 MeV, covering the period of the last ~25 years of CME observations. For a sample of 38 strong SEP events, we first investigate the statistical relations between the recorded peak proton fluxes (I_P) and fluences (F_P) at a set of integral energies of E >10 MeV, E>30 MeV, E>60 MeV, and E>100 MeV versus the projected CME speed near the Sun (V_{CME}) obtained by the Solar and Heliospheric Observatory/Large Angle and Spectrometric Coronagraph (SOHO/LASCO). Based on the inferred relations, we further calculate the integrated energy dependence of both I_P and F_P, assuming that they follow an inverse power-law with respect to energy. By making use of simple physical assumptions, we combine our derived scaling laws to estimate the upper limits for V_{CME}, I_P, and F_P focusing on two cases of known extreme SEP events that occurred on February 23, 1956 (GLE05) and in AD774/775, respectively. Given physical constraints and assumptions, several options for the upper limit V_{CME}, associated with these events, are investigated.
Results. A scaling law relating I_P and F_P to the CME speed as V_{CME}^5 for CMEs ranging between ~3400-5400 km/s is consistent with values of F_P inferred for the cosmogenic nuclide event of AD774/775. At the same time, the upper CME speed that the current Sun can provide possibly falls within an upper limit of $V_{CME} \leq 5500$ km/s.

Key words. solar–terrestrial relations – coronal mass ejections (CMEs) – solar energetic particles (SEPs) – solar activity

1. Introduction

Solar Energetic Particle (SEP) events result from acceleration processes associated with both solar flares and coronal mass ejections (CMEs). SEPs propagate in interplanetary space, mostly, along interplanetary magnetic field (IMF) lines before being observed by spacecraft located in the heliosphere (see Desai & Giacalone 2016; Reames 2021, and references there in). A two-class paradigm classifies the SEP events as impulsive or gradual. The impulsive SEP events are assumed to be associated with solar flares and type III radio bursts and are limited in duration, reach small peak intensities, and have typically narrow emission cones (see, e.g., Reames 2021). The gradual SEP events are most energetic and are assumed to be associated with CMEs and type II radio bursts. They can last for several days, achieving elevated peak fluxes, and have in general a broad cone of emission (see, e.g., Desai & Giacalone 2016). Nonetheless, this paradigm has proven to be a simplified view, further complicated by the association of both strong flares and CMEs with SEPs (Cane et al. 2010; Papaioannou et al. 2016).

The fact that SEPs are driven by CMEs was first discussed by Kahler et al. (1978) who also indicated the close relationship of the CME speed and the peak proton flux of SEPs, highlighting the fact that fast CMEs are more likely to drive shocks that are capable of accelerating energetic particles (see also Kahler 1982, 2001). Such a correlation has been widely investigated and verified since then (e.g., Gopalswamy et al. 2002; Cane et al. 2010; Richardson et al. 2014; Papaioannou et al. 2016; Paassilta et al. 2017; Kihara et al. 2020). The interpretation is that shocks driven by fast CMEs are more likely to accelerate efficiently particles since theoretically the acceleration rate depends on the speed of the shock with respect to the upstream medium (Lee et al. 2012).

Routine CME observations by the Large Angle and Spectrometric Coronagraph (LASCO; Brueckner et al. 1995) onboard the Solar and Heliospheric Observatory (SOHO) have been performed since 1997. These observations have revealed that there is no one-to-one correspondence between X-ray flares and CMEs, since there are many more flares observed than CMEs. However, most CMEs are associated with some level of X-ray flare emission. In particular, Yashiro et al. (2006) (their Fig. 1) demonstrated that the stronger the flare in terms of its peak flux in the 1–8 Å soft X-ray (SXR) wavelength band as measured routinely by the GOES satellites, the more likely it is to be associated with a CME. This results from that fact that

solar eruptive events (i.e., flares and CMEs) do not occur in isolation but in concert as a consequence of corresponding changes in the coronal magnetic field. It is noteworthy that, recently Li et al. (2021) put forward a critical study for the flare–CME relation, showing that it depends on the flare class and the size of the source active region (AR). Moreover, the solar origin of SEPs can almost always (∼94%, Papaioannou et al. 2016) be associated with the occurrence of both SXR flares and CMEs. Some additional SEP events generated at (or even beyond) the west limb of the Sun (Cane et al. 2010) could be associated only with CMEs because flare observations are not posible when they occur on the farside of the Sun. As a result, a wealth of statistical studies point to a relation between SXR flare peak fluxes, near-Sun CME speeds, the achieved peak proton intensities, and the fluences of the resulting SEP events. From recent studies investigating such correlations, it was shown that the most prominent correlation is the one found between the SEP peak proton flux and the speed of the CME (i.e., cc= 0.57 for E> 10 MeV), with a tendency to decrease when considering higher particle energies (i.e., 0.40 for E> 100 MeV, see, e.g. Papaioannou et al. 2016).

Scaling relations of the peak proton flux of SEPs (I_P) to the speed of the CME (V_{CME}) have been proposed by several authors. In particular, Kahler (2001) showed that the relation of the peak proton flux of SEPs at 2 and 20 MeV has a dependence to the V_{CME} of the form $I_P \propto V_{CME}^{4.36}$ & $I_P \propto V_{CME}^{4.83}$, respectively. Investigating 130 SEP events at an integral energy of E>10 MeV and 88 SEP events at an integral energy of E>100 MeV associated with CMEs originating at western longitudes (i.e., W20–W87°), Belov (2017) found dependencies described as $I_P \propto V_n^{4.02\pm0.39}$ and $I_P \propto V_n^{3.01\pm0.50}$, respectively, with $V_n = \frac{V_{CME}}{1000}$[1]. Lario & Karelitz (2014) showed that the SEP peak intensity versus the CME speed follows, in a good approximation, a triangular distribution. This method directly provided *upper* limits to the peak proton particle intensity that can be observed in the prompt component of the SEP events. In particular, these authors showed that for three energy ranges spanning from 9-80 MeV, the resulting *upper* limit dependence scales with $I_P \propto V_{CME}^{\gamma}$ with γ ranging from 4.90-5.63 (see their Figure 5). Takahashi et al. (2016) showed on theoretical grounds that the upper limit for the peak proton flux of E>10 MeV is proportional to the CME speed as $I_P \propto V_{CME}^{5}$.

In our previous study (Papaioannou et al. 2023, – hereafter *part I*), we presented the dependence of SEPs on flare parameters. In particular, we investigated the relationship between the GOES 1–8 Å SXR peak flux (F_{SXR}) of the parent flare versus the SEP event peak proton flux (I_P) and fluence (F_P). We showed that a direct estimation of the upper limit SEP fluence spectra based on F_{SXR} alone is possible and leads to a quantification of the radiation environment. The present follow-up study deals with the dependence of SEPs on the properties of the associated CMEs. With this purpose, we utilize the catalog presented in detail in *part I* (Appendix C) and start with the analysis of the relationships between V_{CME} and I_P, and consider the dependence of V_{CME} on F_{SXR}. Based on the findings of Takahashi et al. (2016), showing that the upper limit for the peak proton flux of E>10 MeV depends on the CME speed as $I_P \propto V_{CME}^{5}$, we derive upper limits and scaling relations among the CME speeds (V_{CME}) and the achieved SEP peak flux (I_P) at each integral energy (from E>10 to E>100 MeV). We then extend these relations to incorporate the fluence (F_P) of SEPs. Additionally, we deduce the upper limit fluence spectra of SEPs based on V_{CME}, whereas in *part I* where the SEP fluence spectra were obtained based on F_{SXR}.

In an attempt to estimate upper limits of the extreme events that can stem from our host star, Gopalswamy et al. (2010), presented calculations based on a hypothetical AR with the largest reported AR area (i.e., 5000 millionths of a solar hemisphere, msh) and the maximum measured sunspot magnetic field (B = 6100 G). These authors then estimated the potential energy of the AR to be 10^{36} erg that could produce a SXR flare of ∼ X1000 class (i.e., $10^{-1} W/m^2$). Consequently, the estimated maximum CME speed associated with the largest solar flare class, taking into account an upper limit of 26% of the potential energy being converted into CME kinetic energy, was found to be 7200 km s^{-1} – exceeding the highest measured CME speed by the SOHO/LASCO by a factor of ∼ 2 (Gopalswamy 2011). By considering the observations used in this work (Section 2), the obtained scaling relations (Section 3) and the upper limits our Sun can produce (Section 4) we estimate the fastest expected CMEs, the worst-case SEP proton fluxes and fluences, and the corresponding SEP spectrum. Implications for the effects of extreme CMEs on the radiation environment and the limits of recent fluence reconstructions on V_{CME} are put forward and discussed.

2. Data sets

We focus on the relations between SEPs and CMEs. We make use of a well-defined catalog of 65 well-connected (W20-90^o) SEP events that were recorded between 1984 and 2017 and extended from E>10 to E>100 MeV. For each event we first identified the prompt peak intensity (in units of protons $cm^{-2}sr{-}1s^{-1}$), defined as the maximum intensity observed shortly after the onset of the event in situ. In this way energetic storm particles or the ESP component were excluded. Furthermore, we calculated the omni-directional fluence (cm^{-2}) (integration over time) and tabulated all results (see Appendix C in *part I*). Since, SOHO/LASCO measured linear CME speeds only started in 1997 the sample used in this work was reduced from 65 to 38 SEP events. The CME speeds and widths were taken from the online CDAW CME catalog[2] (Yashiro et al. 2004).

3. Scaling relations

3.1. SXR flare flux, CME speed, and peak proton fluxes

As a first step, we study the scaling relations between the CME speed (V_{CME}) and the prompt peak proton flux (I_P) for integral energies E> 10 MeV, E> 30 MeV, E> 60 MeV, and E> 100 MeV. Figure 1 shows I_P for E>10 MeV as a function of V_{CME}. The correlation coefficient between I_P and V_{CME} for the SEP events that reach an integral energy of E> 10 MeV is cc=0.51, assuming a linear regression obtained from the Reduced Major Axis (RMA, see discussion in Papaioannou et al. 2023) method, leading to $I_P \propto V_{CME}^{\gamma}$, with γ=3.52±0.59. Additionally, the gray shaded envelope in Fig. 1 provides the estimated error[3].

As discussed in Takahashi et al. (2016), an upper limit for this relation is given by $I_P \propto V_{CME}^{5}$, when passing through the upper-most point of the employed sample. Such a scaling relation, in general, is deduced employing three assumptions: (a) that the CME mass (M_{CME}) is equal to the sum of the gravitational stratified AR corona (see Eq. (1) of Takahashi et al. (2016)), (b)

[1] The normalization employed in that paper does not affect the proportionality

[2] https://cdaw.gsfc.nasa.gov/CME_list/

[3] see Papaioannou et al. (2023) for details on the error estimation

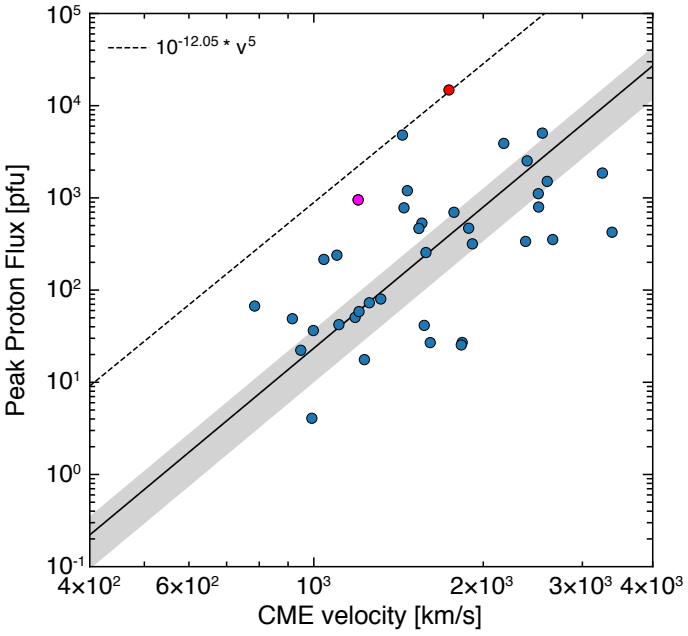

Fig. 1. $I_P \propto V_{CME}^{\gamma}$ relation for E> 10 MeV, with γ=3.52±0.59. The dashed black line corresponds to the upper limit of I_P in terms of V_{CME} with γ=5. The upper point in our sample corresponds to the SEP event on 8 November 2000 (see the relevant Appendix in *part I*) and is used for the scaling. It is labeled with a red dot. In addition, the event on 15 April 2001 is highlighted with a magenta dot (see details in the text).

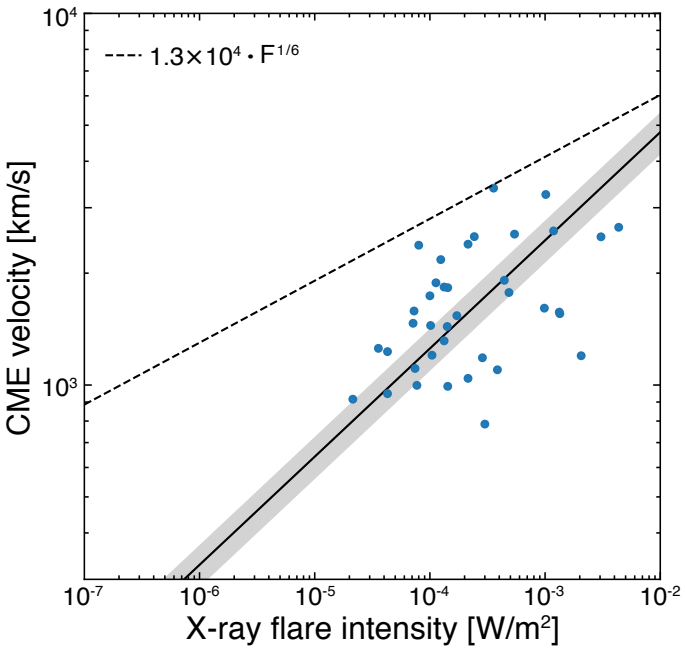

Fig. 2. Relation between CME velocity (V_{CME}) and the flare SXR peak flux (F_{SXR}). The solid black line represents the linear RMA regression fit $V_{CME} \propto F_{SXR}^{\alpha}$ with α = 0.43±0.08. The dashed black line corresponds to the upper limit of V_{CME} in terms of F_{SXR}. See text for details.

the CME kinetic energy (E_{CME}) is proportional to the total energy released during a flare, which is also a fraction f of the AR magnetic field energy (see e.g. Emslie et al. 2012; Papaioannou et al. 2023) (see Eq. (2) of Takahashi et al. 2016), and (c) the total kinetic energy of SEPs (E_p) is proportional to flare energy, and the duration of the proton flux enhancement is determined by the CME propagation timescale $t_{CME} \propto L/V_{CME}$ (L being the length scale of the flaring AR) which leads to a scaling relation of $I_P \propto V_{CME}^5$. Based on our sample, we derive this upper limit to be at $I_P = 10^{-12.05} \cdot V_{CME}^5$ (dashed black line in Fig. 1). The event that marks the upper limit fit is the event on 8 November 2000 SEP (indicated by a red dot in Fig. 1). We further highlighted the ground-level enhancement event of 15 April 2001 (GLE60) in magenta (see details in Appendix B).

A scatter plot between V_{CME} and the flare SXR peak flux (F_{SXR}) is presented in Fig. 2. The RMA regression is quantified as $V_{CME} \propto F_{SXR}^{0.43\pm0.08}$ with a correlation coefficient of cc=0.43. Takahashi et al. (2016) suggested that the upper limit of this relation is given by $V_{CME} \propto F_{SXR}^{1/6}$. Following the description by Takahashi et al. (2016), based on our sample, we find the relation to be $V_{CME} = 1.3 \times 10^4 \cdot F_{SXR}^{1/6}$ (dashed black line in Fig. 2), passing by the point with the highest V_{CME} = 3387 km/s corresponding to the event on 10 November 2004.

The results presented up to this point assume statistical relations among the SXR peak flux of flares (F_{SXR}), the speed of the CME (V_{CME}), and the peak proton flux (I_P) at an integral energy of E>10 MeV (e.g. Takahashi et al. 2016). Both solar flares and CMEs are drivers of SEP events (e.g. Cane et al. 2010). Hence a correlation between V_{CME}, F_{SXR} and I_P has often been put forward (e.g. Papaioannou et al. 2016). Nonetheless, previous findings have solely been derived from an E> 10 MeV sample of SEPs. Although neglected in most studies, here, we further investigate solar scaling relations for the integrated E>30 Mev, E> 60 Mev, and E> 100 MeV energy channels based on the same methodology. As a result, scaling relations $I_P \propto V_{CME}^{\gamma}$ are obtained for each of these integral energies (see Appendix A). Our results are presented in Fig. A.1, where the $I_P - V_{CME}$ relations for E>30 MeV (top panel), E> 60 MeV (middle panel), and E> 100 MeV (bottom panel) are displayed. Table 1 summarizes the slopes obtained by the RMA regression fits for each case.

Table 1. Slopes of the relations obtained for the peak proton flux (I_P) to the CME speed (V_{CME}), and the corresponding correlation coefficients for each integral energy, derived in this work.

Integral Energy (MeV)	**Slope I_P-V_{CME} (γ)**	**Correlation coefficient (cc)**
E > 10	5.09±0.78	0.58
E > 30	5.24±0.84	0.54
E > 60	5.35±0.94	0.44
E > 100	5.52±1.02	0.38

The power-law index γ presents a relatively slight increase with energy, varying between 5.09 ± 0.78 at E>10 MeV up to 5.52 ± 1.02 at E>100 MeV, while also showing a consequent slight increase of the uncertainties. At the same time, the correlation coefficients of the $I_P - V_{CME}$ relation seem to decrease with energy.

3.2. Establishing the relations

According to Takahashi et al. (2016), utilizing the argumentation by Emslie et al. (2012), assuming that the CME mass is the sum of the mass within gravitationally stratified AR corona; the kinetic energy of CMEs is proportional to the flare energy ($E_{CME} \propto E_{flare}$) and that the energetic proton flux in response to the SXR class of flares can be estimated under the assumption that F_{SXR} is roughly proportional to the total energy released during flares, i.e., $F_{SXR} \propto E_{flare}$ (consistent with the observational

findings in Emslie et al. (2012)), V_{CME} is scaled with F_{SXR} as:

$$V_{CME,upper} = V_0 \cdot F_{SXR}^{1/6}(km/s), \quad (1)$$

with F_{SXR} normalized in units of 1 W/m^2 and $V_0 = 1.3 \cdot 10^4$ km/s, as derived from our sample. Equation (1) is shown as a dashed black line in Fig. 2.

Moreover, as outlined in Takahashi et al. (2016) and here above, assuming that the total kinetic energy of protons in SEP events (E_P) is proportional to the flare energy (E_{flare}) and that the duration of the proton flux enhancement is determined by the CME propagation timescale t_{CME} it follows that $E_P \propto I_P \cdot t_{CME} \propto E_{flare}$. Therefore, I_P is scaled with V_{CME} as:

$$I_{P,upper} \propto V_{CME}^5. \quad (2)$$

The relations for each integral energy are positioned to run through the strongest SEP events of our sample so that we can discuss the upper limits of the CME velocity ($V_{CME,upper}$) and peak proton flux ($I_{P,upper}$) in each plot of Figs. 1 and A.1.

4. Estimating the CME speed, peak proton flux, and fluence for solar extreme events

4.1. Upper limits

4.1.1. Estimation of $V_{CME,upper}$

Figure 3 is similar to Fig. 2 and shows a scatter plot between V_{CME} and F_{SXR}, with the RMA fit (solid black line) embedded into the gray error band and the upper limit deduced from Eq. (1), presented as a dashed black line. The investigation for the upper limit of the V_{CME} is based on the SXR peak flux of the associated solar flare together with Eq. (1). Considering the F_{SXR} values estimated by Cliver et al. (2022) of X400±200 (i.e., 4×10^{-2} W/m^2 $\pm$ 2×10^{-2} W/m^2) for the AD774/775 SEP event and X28±14 (i.e. 2.8×10^{-3} W/m^2 ±1.4×10^{-3} W/m^2) for GLE05, we obtained $V_{CME,upper} =\sim 7600\ ^{+534}_{-827}$ km/s and $V_{CME,upper} =\sim 4880^{+342}_{-532}$ km/s for GLE05. For more details on the F_{SXR} ranges see Cliver et al. (2022) and Papaioannou et al. (2023).

In the next step, known published scaling relations of V_{CME} are investigated and compared with our findings. Gopalswamy (2018) has shown that the largest expected CME speed might be as high as ~ 7200 km/s. This estimate is based on extreme solar conditions that differ from those of the current Sun . Interestingly, Fig. 7(a) of Gopalswamy (2018) provides an estimation of V_{CME} and an upper limit ($V_{CME,upper}$) based on the magnetic potential energy (MPE [erg]) of active regions (ARs), giving the corresponding empirical relations as

$$V_{CME} = 748 \cdot \log(\mathrm{MPE}) + 636(\mathrm{km/s}), \quad (3)$$

which represents the whole sample of CMEs and ARs considered by Gopalswamy (2018) and

$$V_{CME,upper} = 1136 \cdot \log(\mathrm{MPE}) + 1557(\mathrm{km/s}), \quad (4)$$

which is extracted from the highest values of the Goplaswamy sample, leading to the upper limit $V_{CME,upper}$.

Following Emslie et al. (2012), the bolometric flare energy is related to MPE by $F_{TSI} = 0.025 \cdot MPE$ or vice versa $MPE = 40 \cdot F_{TSI}$. Using our 38 SEP events (see Appendix C of *part I*), the F_{SXR} was first substituted in Eq. (1) of Cliver et al. (2020), translating F_{SXR} to F_{TSI} for each flare. From the above relation, the MPE is estimated. Once calculated for each case, the expected CME speeds and its upper limit of our sample was

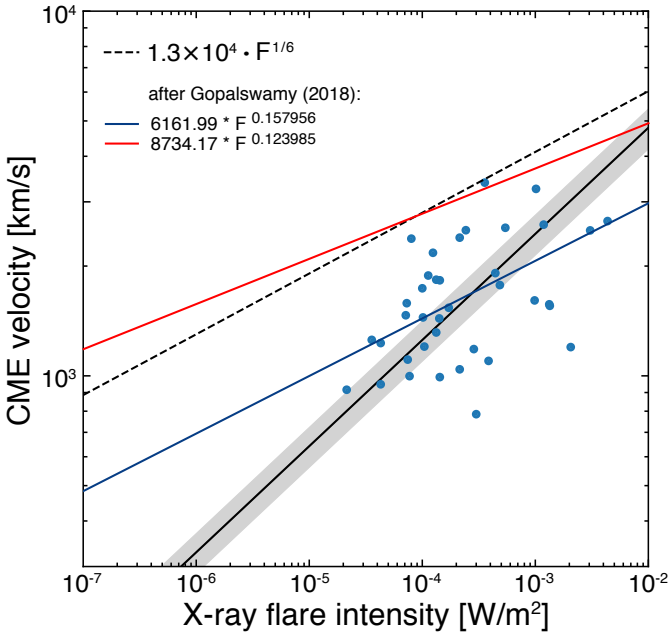

Fig. 3. Similar to Fig. 2 with the addition of Eq. (5) (blue line) and Eq. (6) (red line).

derived utilizing Eqs. (3) and (4). The obtained data were subsequently used to obtain fits of V_{CME} ($V_{CME,upper}$) *vs* F_{SXR} which were then added to Fig. 2 obtaining the representation in Fig 3. Thereby, the obtained fits are given by

$$V_{CME} = 6162 \cdot F_{SXR}^{0.158} \left[\sim 6.2 \times 10^3 \cdot F_{SXR}^{1/6}\right](km/s), \quad (5)$$

with F_{SXR} normalized in units of 1 W/m^2 and 6.2×10^3 in km/s. This relation provides the $V_{CME} \propto F_{SXR}$ relation presented as a blue line in Fig. 3 and

$$V_{CME,upper} = 8734 \cdot F_{SXR}^{0.124} \left[\sim 8.7 \times 10^3 \cdot F_{SXR}^{1/8}\right](km/s), \quad (6)$$

with F_{SXR} normalized in units of 1 W/m^2 and 8.7×10^3 in km/s. This relation provides the $V_{CME,upper} \propto F_{SXR}$ relation presented as a red line in Fig. 3.

Table 2 shows that $V_{CME,upper}$, for the extreme cases of AD774/775 and GLE05, derived from Eq. (1) (Fig.3; dashed black line), leads to ~1.13-1.32 times higher CME speeds than those obtained by Eq. (6) (red solid line in Fig.3). Nonetheless, Fig. 3 shows that Eq. (6) is inclusive of all 38 SEP events, except for the 10 November 2004 one, of our sample and provides an alternative upper limit for the CME speed, compared to that proposed by Takahashi et al. (2016) (i.e. the dashed black line in Fig. 3). Evidently, due to the difference of the obtained slopes (i.e., red line vs dashed black), the difference will be larger for stronger, i.e., extreme flares. In other words, the stronger the flare in terms of F_{SXR}, the larger the difference for the different estimates of $V_{CME,upper}$. At the same time, Eq. (5) (blue solid line in Fig.3) has a similar slope as Eq. (1) but with a lower scaling. Thus, the blue line underestimates the CME speed, especially for M- and X-class flares of our sample, but provides a statistically deduced representation of the expected V_{CME}, in agreement with Fig. 7(a) of Gopalswamy (2018).

4.1.2. SEP peak fluxes (I_P) and fluences (F_P) driven by V_{CME}

Here the relation between I_P, F_P and V_{CME} is further investigated. In particular, the upper limit peak proton flux was calcu-

Table 2. *Upper limit* CME speeds ($V_{CME,upper}$, [km/s]) for the SEP event on AD774/775 and GLE05 derived in this work (i.e. from Eq. (1) and Eq. (6)) while Eq. (5) provides the V_{CME} for each event.

	AD774/775	GLE05	Fig.3
Equation	**CME speed – V_{CME} (km/s)**		**line**
Eq. (1)	7602^{8134}_{6773}	4881^{5222}_{4348}	dashed
Eq. (6)	5860^{6162}_{5377}	4214^{4431}_{3867}	red
Eq. (5)	3706^{3951}_{3322}	2435^{2596}_{2182}	blue

lated utilizing the $I_P = V_{energy} \cdot V_{CME}^5$ relations (where V_{energy} are the coefficients used in the dashed black lines on Fig. 1 and Fig. A.1 for all integral SEP energies employed in this work). Similar to *part I*, from the established upper limit relation of the peak proton flux, $I_{P,upper}$, the corresponding upper limit of the fluence $F_{P,upper}$ can also be retrieved. In this case, as a function of V_{CME} as:

$$F_{P,upper} = F_{P,energy} \cdot (V_{energy} \cdot V_{CME}^5)^{\delta} \quad (7)$$

with $F_{P,energy}$ and δ directly taken from Table A.1 of Papaioannou et al. (2023)[4] and V_{energy} being: $V_{E10} = 10^{-12.05}$, $V_{E30} = 10^{-12.55}$, $V_{E60} = 10^{-13.14}$, $V_{E100} = 10^{-13.65}$. V_{energy} for each integral energy considered is scaled with $(km/s)^{-5}$.

The corresponding outputs are presented in Appendix B. Figure B.1 shows the F_P vs. V_{CME} relation obtained for our sample of 38 SEP events, for which CME information was available, using the RMA regression fit (solid black lines) for each integral energy embedded in a gray error-envelope. The dashed black lines correspond to the *upper* limits from Eq. (7).

In order to investigate the effect of $V_{CME,upper}$ and V_{CME} on the calculation of I_P and F_P the outputs from Eq. (1), Eq. (6), and Eq. (5) (see Table 2) were used. Using these values (incl. upper/lower limits), the peak proton flux was derived employing the $I_P \propto V_{CME}^5$ relations (Figs. 1 and A.1), whereas the fluence was calculated by substituting V_{CME} (or $V_{CME,upper}$) in Eq. (7).

The obtained results are provided for both the upper limit peak proton flux and fluence in Tab. B.1 showing that the *upper limit* I_P - calculated when using $V_{CME,upper}$ from Eq. (1) and Eq. (6)- differ by a factor of ∼2.5. The corresponding $F_{P,upper}$ by a factor of ∼3.0. At the same time, the obtained I_P and F_P are lower than the upper limits by a factor of ∼40 when V_{CME} from Eq. (5) is used as input.

4.2. V_{CME} and its upper limit

The *upper limit* of V_{CME} obtained from Eq. (1) leads to a maximum value of ∼7600 km/s for an X425 SXR flare associated with the AD774/775 SEP event. This CME speed agrees with the value of ∼7200 km/s reported by Gopalswamy (2011). However, such a high CME speed requires extreme conditions (i.e., B=6100 G over the full sunspot region) that are difficult to reconcile with the current Sun. Moreover, the RMA fit for the same case (see black solid line in Fig. A.1) leads to values of ∼12000 km/s (for the same SXR flare of X425), which is even more difficult to present with the inherent limitations imposed by the energetics of our Sun and thus unrealistic. Adding to this, it was shown that V_{CME} from Eq. (6) provides maximum values for the SXR flare associated to the AD774/775 event of 5300-6100 km/s, but that falls to ∼ 3300-3900 km/s when utilizing Eq. (5) (see Table 2 and Figure 3).

During the modern era of CME measurements, the Sun produced a SEP event on 4 November 2003, associated with an X28 (X43.2[5]) solar flare and a CME with a linear speed of 2657 km/s[6]. However, for the determination of the CME speed of this event, only three points were used in the LASCO field of view. Additionally, the CME emerged under distorted conditions, which complicates the speed estimates. Moreover, Gopalswamy et al. (2005) suggested that the maximum V_{CME} of our host star may not be much higher than ∼3000 km/s.

Figure 4 shows our results of the F_P - V_{CME} dependence for E>30 MeV. In each panel we added the fluence of the extreme and rare SEP events found in the cosmogenic radionuclide records (e.g., Miyake et al. 2012; Mekhaldi et al. 2015; Brehm et al. 2021; Mekhaldi et al. 2021): the AD993 (upper left), AD774/775 (upper right), 660 BCE (lower left) and 7176 BCE (lower right). For these selected events, we use the recent fluence reconstructions put forward by Koldobskiy et al. (2023). Thus far, when utilizing the obtained fluence range for each of these events (Y-axis in each panel), the V_{CME} range leading to this fluence can be directly obtained utilizing the *upper limit* scaling law (dashed black line). Similar figures were constructed for E>60 MeV (Figure C.1) and E>100 MeV (Figure C.2). When utilizing the *upper limit*, the range of CME speed forsuch extreme SEPs falls within a mid-mean range of 3241 - 5255 km/s based on all integral energies (i.e., see details in Appendix C and Table C.1).

4.3. Spectrum based on V_{CME}

The top panel of Fig. 5 provides the obtained integral fluence spectra of the AD774/775 event, for the three different estimates of the CME speed based on the F_{SXR} (see Table 2). In particular, the upper limit of V_{CME} was obtained by Eq. (1) (dashed black line in Fig. 3), Eq. (5) (blue solid line in Fig. 3), and Eq. (6) (red solid line in Fig. 3). Thereafter, the F_P - V_{CME} relations (i.e., RMA fits in Fig.B.1 and Eq. (7) for the upper limits) were employed to identify the expected fluence at the respective integral energies. The solid black, blue, and red lines are obtained via the inverse power-law fit of the estimated fluences per integral energy of the uppermost points included in Table B.1. These points are calculated using Eq. (7). For each of the three fits, the shaded area provides the 1-σ error. Estimates of the energy-dependent fluences of the AD774/775 event, independently obtained by Usoskin et al. (2021) and Koldobskiy et al. (2023) are included as blue and black squares, respectively.

The obtained integral fluence spectra displayed in the top panel of Fig. 5 are driven by the associated V_{CME}. The reconstructions by Usoskin et al. (2021) and Koldobskiy et al. (2023) seem to fall above the estimated fluence spectra obtained from an X425±175 flare converted to V_{CME} using Eq. (5) (i.e., solid blue line) and below the upper limit (V_{CME}^5) spectra presented in this work (i.e., solid black and red lines) when converting the same flare magnitude using Eq. (1) and Eq. (6), respectively. Therefore, the obtained *upper* limit (i.e., "worst case") fluence spectra in these two later cases (solid black and red lines respectively) seem to be restrictive to the actual fluence reconstructed values in the case of AD774/775. Nonetheless, for higher energies (i.e.,

[4] https://www.aanda.org/articles/aa/full_html/2023/03/aa43407-22/T4.html

[5] see recent re-calibration in Hudson et al. (2024)

[6] https://cdaw.gsfc.nasa.gov/CME_list/sepe/

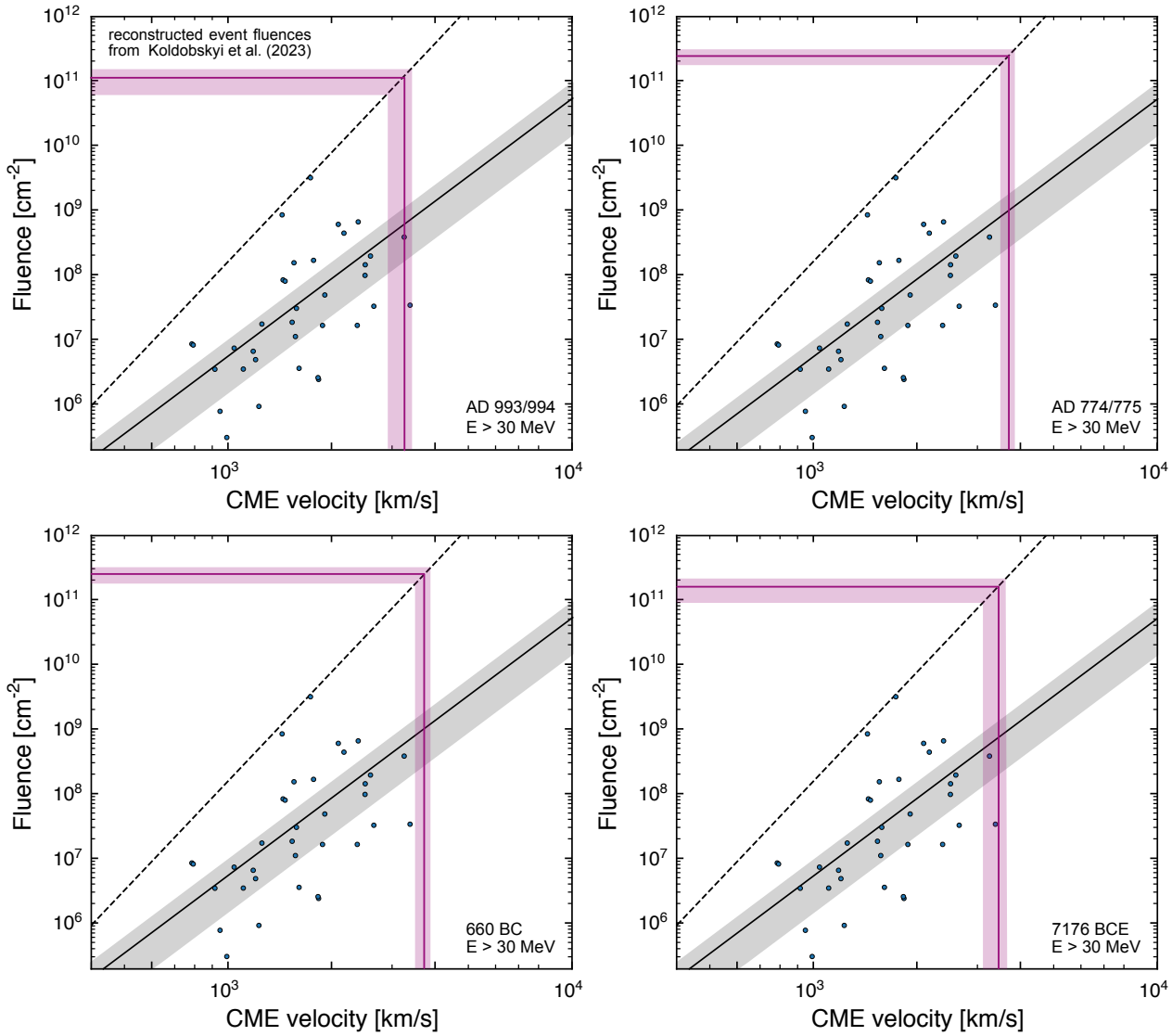

Fig. 4. F_P-V_{CME} relations for E>30 MeV. The magenta ribbons on the Y-axis correspond to the F_P range for AD993, AD774/775, 7176 BCE, and 660 BCE (in the clockwise direction) as published by Koldobskiy et al. (2023). The ribbons on the X-axis show the estimated V_{CME} range for the events based on the RMA fit (black solid line) and the upper limit (worst case scenario; dashed black lines).

E>430 MeV and E>1000 MeV), the difference between the actual estimates of the fluence (black squares) and the obtained fluence spectra (solid black line) exceeds one order of magnitude, which suggests that a CME speed of 7602 $^{+532}_{-829}$ km/s overestimates the fluence at these energies.

The bottom panel of Fig. 5 is similar to the top panel. However, here, the obtained fluence spectrum assumes a V_{CME} range of 3421 km/s (lower limit) to 5482 km/s (upper limit) as obtained in Appendix C (magenta band). It shows that the independently obtained fluence estimates of Usoskin et al. (2021) and Koldobskiy et al. (2023) fall well within the estimated fluence range for energies between E>30MeV and E>1 GeV. Assuming that the AD774/775 event is one of the strongest events ever recorded (based on our current knowledge), the fluence spectra depicted in the bottom panel of Fig. 5 offers an upper limit ("worst case") fluence, inclusive of the independently obtained fluence values, utilizing a CME speed of 5482 km/s (see Appendix C for more detail). Thus, in turn, a CME speed of ≤5500 km/s could be restrictive for our current Sun.

5. Conclusions

In this paper, we investigated the dependence of SEP events on V_{CME}. In particular, the scaling relations that describe I_P, V_{CME} and F_P seem to be consistent with statistical relations obtained by observations. These have been extended from E>10 MeV up to E>100 MeV. Based on the presented analysis, we derived the maximum expected CME speed associated with the largest estimated F_{SXR} flare unleashed by the Sun (i.e., X600) to range between ~3950 and ~8134 km/s depending on the underlying relation (see Table 2). However, a CME speed as high as ~8200 km/s could only result from exceptional and most likely unrealistic conditions (see Gopalswamy 2018).

Moreover, the use of Eq. (5) showed that a CME speed in the order of ~3950 km/s, which is in relative agreement with CME observations of the extreme case of 4 November 2001 (V_{CME}=2660 km/s). Such V_{CME} provides an upper limit fluence spectrum that is consistent with observations for E>30 MeV (blue line in Fig. 5, top panel). However at higher energies from E>60MeV to E>430 MeV such CME speed leads to an underestimation of the fluence. At the same time, the use of Eq. (6)

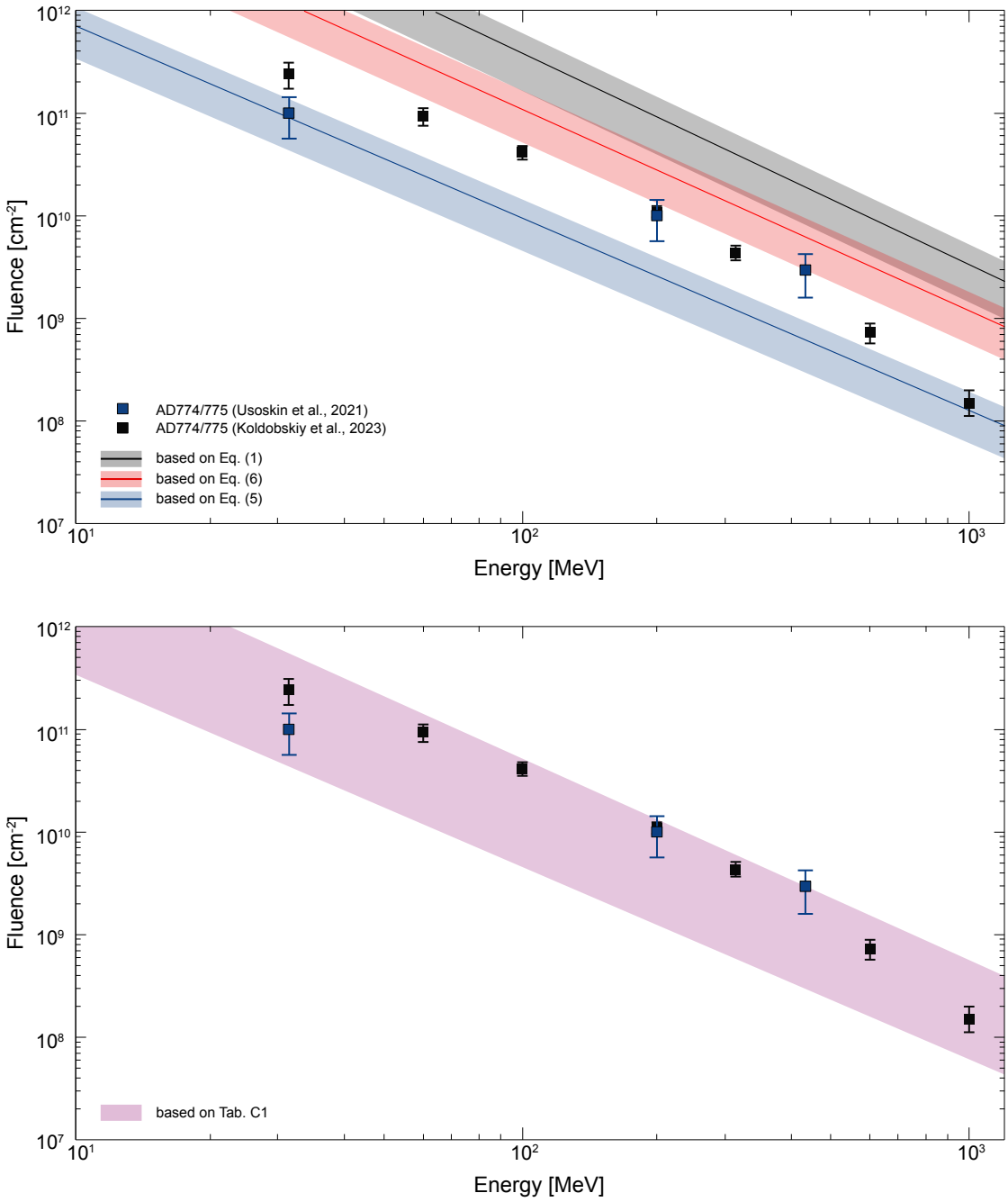

Fig. 5. SEP fluence spectra obtained from the scaling relation F_P-V_{CME} for AD774/775. Each solid line is the inverse-power law fit to the obtained integral fluence values acquired when utilizing V_{CME} from Table 2 (top panel) and the range of CME speeds obtained from Table C.1 (bottom panel). The derived AD774/775 fluences by Usoskin et al. (2021) and Koldobskiy et al. (2023) are shown as filled blue and black squares, respectively.

showed that a CME speed in the order of ~5380 km/s, provides an upper-limit spectrum comparable with higher energies (i.e., E>100 MeV, E>200 MeV & E>430 MeV), although overestimating the respective fluence. Nonetheless, at E>30 MeV, an upper-limit estimation of the fluence for AD774/775 based on V_{CME} ≤4000 km/s seems to be a better representative of the obtained fluence (Usoskin et al. 2021).

The scaling relations presented in this study provide a direct estimate of the upper limit peak flux (I_P) and fluence (F_P) based on the V^5_{CME} relation driven by the associated CME speed. Both F_{SXR} and V_{CME} show correlation coefficients of roughly similar strength (see Papaioannou et al. 2023, and this work). However, F_{SXR} possibly provides more robust estimates of I_P and F_P than the CME speed because (a) the CME speed measurement is more uncertain and may be strongly variable during the early phase close to Sun (Zhang et al. 2001; Vršnak 2008) with peak accelerations as high as 10 km/s^2 (Bein et al. 2011; Veronig et al. 2018) whereas the flare peak SXR flux (F_{SXR}) is well measured [7], and (b) the conversion of the F_{SXR} to the V_{CME} (Fig. 3) leads to three CME speed estimations for the same flare, depending on which relation is considered. Based on this and the scaling rela-

[7] One major reason is the projection effects, which depend on the location of the source region on the Sun (Paouris et al. 2021).

tions presented in (*part I*, Papaioannou et al. 2023), F_{SXR} is almost linearly scaled ($\gamma = 5/6$) to I_P and F_P, whereas V_{CME} scales with a $\gamma = 5$. As a result, errors in determining the CME speed are strongly enhanced pertaining to the dependent quantity upon calculations. This spread of values obtained for fluences driven by the same CME speed (see Fig. 4) could also be explained by the apparent lack of V_{CME} values that extend to $\geq$ 4000 km/s, which results in a critical gap not being covered by (any of) the sample(s) used (at any such study). Additionally, one of the theoretical assumptions is that the relation $t_{CME} \propto L/V_{CME}$, with L being the AR size, holds true. However, for completeness it should be noted that if a constant length L_0 is assumed instead, the scaling relation changes to $F_P \propto V_{CME}^7$. Although plausible for the acceleration of particles whose length scales are independent of the AR size, such a scaling law would in fact mean that even slower CMEs would result to extreme fluences (orders of magnitude higher) at the respective energies employed in this work. Based on the measurements of CMEs of the last 27 years, this seems highly unlikely.

The top panel of Fig. 5 shows that the highest expected fluence for a given V_{CME} can not (or slightly) overcome values obtained by the red line. In addition, the bottom panel of Fig. 5 highlights that applying the scaling relation $F_P \propto V_{CME}^5$ and assuming CME speeds between 3420 km/s and 5480 km/s leads to F_P values for one of the largest SEP event marked until this day (i.e., AD774/775) that are in good agreement with the calculated values by Usoskin et al. (2021) and Koldobskiy et al. (2023).

It should be highlighted that such relations do not necessarily assume pure solar flare or CME acceleration of SEPs. As noted in the pioneering work by Emslie et al. (2012), there is an interplay between X-ray and SEP emission in complex solar events, including CME generation, so that the energy release is distributed between radiation and accelerated particles. Moreover, scaling relations are inherent of caveats and limitations, as outlined in *part I*; (Papaioannou et al. 2023) but provide valuable content for the estimation of the worst case radiation environment based on the V_{CME} alone.

Our results may apply to other Sun-like stars. Nonetheless, for our host star, Li et al. (2021) provided an estimate that no more than 50% of solar flares with magnitude ~X100 would generate CMEs caused by the strong magnetic confinement exerted on flares/eruptions from the largest ARs in terms of their overall magnetic flux. Naturally, this finding has consequences for the rate of SEP production. Nevertheless, as highlighted in *part I* and Sec.1, scaling relations offer valuable context for a worst-case (upper limit) estimate of the radiation environment since such relations inherently assume flares to be associated with CMEs and consequently with SEP events. However, this one-to-one association scenario is unrealistic and not observed on the Sun since tens of thousands of flares result in only a few hundred SEP events (Papaioannou et al. 2016). This finding was recently corroborated by the study of Kahler & Ling (2023), who concluded that one may not directly use scaling relations without taking this imbalance into account.

Our work has further underlined the difficulties in identifying the upper CME speed and how this impacts the resulting I_P and F_P values. In addition, one should note that caution is needed in the case of stellar CMEs since there is an observational gap in the stellar regime: while numerous stellar flares have been observed in Sun-like stars, stellar CMEs might be rare and - so far - cannot be directly observed (see details in Moschou et al. 2019; Leitzinger & Odert 2022). Nonetheless, recent studies demonstrated a different approach for identifying stellar CMEs on cool stars, based on sudden dimmings in the extreme ultraviolet (EUV) and X-ray emission caused by the CME mass loss (Veronig et al. 2021; Loyd et al. 2022; Notsu et al. 2024), showing potential for future research efforts.

Acknowledgements. The authors would like to thank the anonymous referee for a critical and constructive reading of the manuscript and for valuable comments that improved the contents of the paper. AP, KH, and DL acknowledge the International Space Science Institute and the supported International Team 441: *High EneRgy sOlar partICle Events Analysis (HEROIC)*. KH acknowledges the support of the DFG priority program SPP 1992 "Exploring the Diversity of Extrasolar Planets (HE 8392/1-1)". AP and KH also acknowledge the supported International Team 464: *The Role Of Solar And Stellar Energetic Particles On (Exo)Planetary Habitability (ETERNAL)*. AP and DL acknowledge support from NASA/LWS project NNH19ZDA001N-LWS. DL also acknowledges support from project NNH17ZDH001N-LWS. AMV acknowledges the Austrian Science Fund (FWF): project no. 10.55776/I4555.

References

Bein, B. M., Berkebile-Stoiser, S., Veronig, A. M., et al. 2011, ApJ, 738, 191
Belov, A. V. 2017, Geomagnetism and Aeronomy, 57, 727
Brehm, N., Christl, M., Adolphi, F., et al. 2021, Nature Geoscience, 14, 10
Brueckner, G. E., Howard, R. A., Koomen, M. J., et al. 1995, Sol. Phys., 162, 357
Cane, H. V., Richardson, I. G., & von Rosenvinge, T. T. 2010, Journal of Geophysical Research (Space Physics), 115, A08101
Cliver, E. W., Hayakawa, H., Love, J. J., & Neidig, D. F. 2020, ApJ, 903, 41
Cliver, E. W., Schrijver, C. J., Shibata, K., & Usoskin, I. G. 2022, Living Reviews in Solar Physics, 19, 2
Desai, M. & Giacalone, J. 2016, Living Reviews in Solar Physics, 13, 1
Emslie, A. G., Dennis, B. R., Shih, A. Y., et al. 2012, ApJ, 759, 71
Gopalswamy, N. 2011, in Astronomical Society of India Conference Series, Vol. 2
Gopalswamy, N. 2018, in Extreme events in geospace (Elsevier), 37–63
Gopalswamy, N., Akiyama, S., Yashiro, S., & Mäkelä, P. 2010, in Magnetic Coupling between the Interior and Atmosphere of the Sun, ed. S. Hasan & R. J. Rutten (Berlin, Heidelberg: Springer Berlin Heidelberg), 289–307
Gopalswamy, N., Yashiro, S., Liu, Y., et al. 2005, Journal of Geophysical Research: Space Physics, 110
Gopalswamy, N., Yashiro, S., Michałek, G., et al. 2002, ApJ, 572, L103
Hudson, H., Cliver, E., White, S., et al. 2024, Sol. Phys., 299, 39
Kahler, S. W. 1982, J. Geophys. Res., 87, 3439
Kahler, S. W. 2001, J. Geophys. Res., 106, 20947
Kahler, S. W., Hildner, E., & Van Hollebeke, M. A. I. 1978, Sol. Phys., 57, 429
Kahler, S. W. & Ling, A. G. 2023, ApJ, 956, 24
Kihara, K., Huang, Y., Nishimura, N., et al. 2020, ApJ, 900, 75
Koldobskiy, S., Mekhaldi, F., Kovaltsov, G., & Usoskin, I. 2023, Journal of Geophysical Research (Space Physics), 128, e2022JA031186
Lario, D. & Karelitz, A. 2014, Journal of Geophysical Research (Space Physics), 119, 4185
Lee, M. A., Mewaldt, R. A., & Giacalone, J. 2012, Space Sci. Rev., 173, 247
Leitzinger, M. & Odert, P. 2022, Serbian Astronomical Journal, 205, 1
Li, T., Chen, A., Hou, Y., et al. 2021, ApJ, 917, L29
Loyd, R. O. P., Mason, J. P., Jin, M., et al. 2022, The Astrophysical Journal, 936, 170
Mekhaldi, F., Adolphi, F., Herbst, K., & Muscheler, R. 2021, Journal of Geophysical Research: Space Physics, 126, e2021JA029351, e2021JA029351 2021JA029351
Mekhaldi, F., Muscheler, R., Adolphi, F., et al. 2015, Nature communications, 6, 1
Miyake, F., Nagaya, K., Masuda, K., & Nakamura, T. 2012, Nature, 486, 240
Moschou, S.-P., Drake, J. J., Cohen, O., et al. 2019, ApJ, 877, 105
Notsu, Y., Kowalski, A. F., Maehara, H., et al. 2024, The Astrophysical Journal, 961, 189
Paassilta, M., Raukunen, O., Vainio, R., et al. 2017, Journal of Space Weather and Space Climate, 7, A14
Paouris, E., Vourlidas, A., Papaioannou, A., & Anastasiadis, A. 2021, Space Weather, 19, e2020SW002617
Papaioannou, A., Herbst, K., Ramm, T., et al. 2023, A&A, 671, A66
Papaioannou, A., Sandberg, I., Anastasiadis, A., et al. 2016, Journal of Space Weather and Space Climate, 6, A42
Reames, D. V. 2021, Solar Energetic Particles. A Modern Primer on Understanding Sources, Acceleration and Propagation, Vol. 978
Richardson, I. G., von Rosenvinge, T. T., Cane, H. V., et al. 2014, Sol. Phys., 289, 3059
Takahashi, T., Mizuno, Y., & Shibata, K. 2016, ApJ, 833, L8

Usoskin, I., Koldobskiy, S., Kovaltsov, G., et al. 2021, in Proceedings of 37th International Cosmic Ray Conference — PoS(ICRC2021), Vol. 395, 1319
Veronig, A. M., Odert, P., Leitzinger, M., et al. 2021, Nature Astronomy, 5, 697
Veronig, A. M., Podladchikova, T., Dissauer, K., et al. 2018, ApJ, 868, 107
Vršnak, B. 2008, Annales Geophysicae, 26, 3089
Yashiro, S., Akiyama, S., Gopalswamy, N., & Howard, R. A. 2006, ApJ, 650, L143
Yashiro, S., Gopalswamy, N., Michalek, G., et al. 2004, Journal of Geophysical Research (Space Physics), 109, A07105
Zhang, J., Dere, K. P., Howard, R. A., Kundu, M. R., & White, S. M. 2001, ApJ, 559, 452

Appendix A: The I_P versus V_{CME} relations for different integral energies

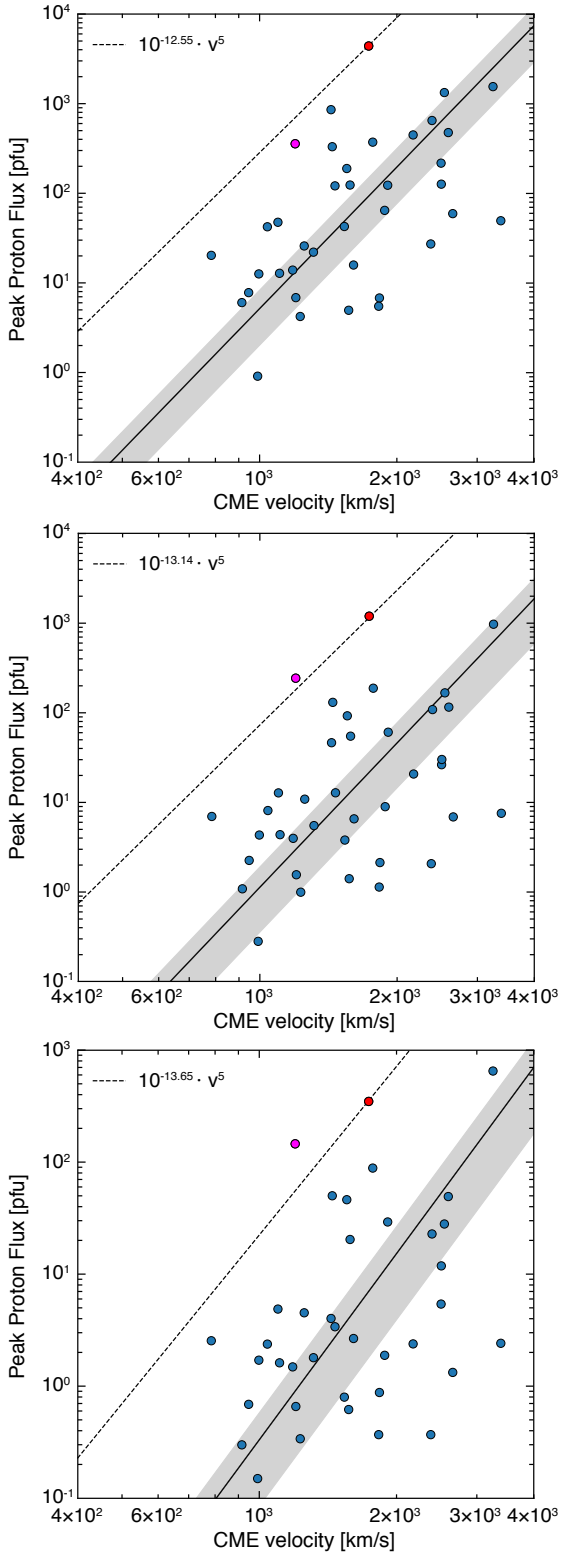

Fig. A.1. Similar to Fig. 1. From top to bottom, these panels present results for E>30-; E>60-, and E>100 MeV, respectively. In all panels, the red dot corresponds to the 8 November 2000 outstanding large SEP event (see text for further details).

Here, we present the same scatter plots as for Fig. 1 but for *IP* at energies E>30 MeV, E>60 MeV, and E>100 MeV. The red and magenta dots indicate the events on 8 November 2000 and 15 April 2001, respectively. Our scaling is based on the 8 November 2000 event. This is the event that achieves the highest peak proton flux across all energies considered (i.e. E>10 - E>100 MeV). From the interplay of the associated V_{CME} with the achieved peak proton flux, the 8 November 2000 SEP event is clearly distinguished at E>10 MeV (Fig. 1) and E>30 MeV (Fig. A.1, top panel). For E>60 MeV the 15 April 2001 SEP event falls on the upper-limit scaling deduced by the 8 November 2000 SEP event (Fig. A.1, dashed black line in the middle panel). However, for E>100 MeV, although the achieved peak proton flux on 15 April 2001 is lower than that of the 8 November 2000 SEP event (Fig. A.1, bottom panel; y-axis) this SEP event is associated to a CME with a speed of 1199 km/s - which is lower than the CME speed of 1738 km/s associated with the 8 November 2000 SEP event. As a result, the magenta point seems to differentiate from the upper-limit scaling (dashed black line) by a factor of ∼2.6. Nonetheless, for consistency and in line with *part I* (see Appendix B of that work) we keep the upper-limit scaling bound to the 8 November 2000 SEP event (red dot) across all energies and propagate the relative error imposed by the differentiation at E>100 MeV to our calculations.

Appendix B: The F_P versus V_{CME} relations

Figure B.1 depicts the F_P-V_{CME} relation obtained for our sample of 38 SEP events for which CME information was available. The RMA regression fit is presented as a solid black line at each integral energy (i.e. panel) embedded in a gray error-envelope. The dashed black lines represent the upper-limits obtained by using Eq. (7). In each case, the obtained dashed black line yields an upper-limit to the observed fluences.

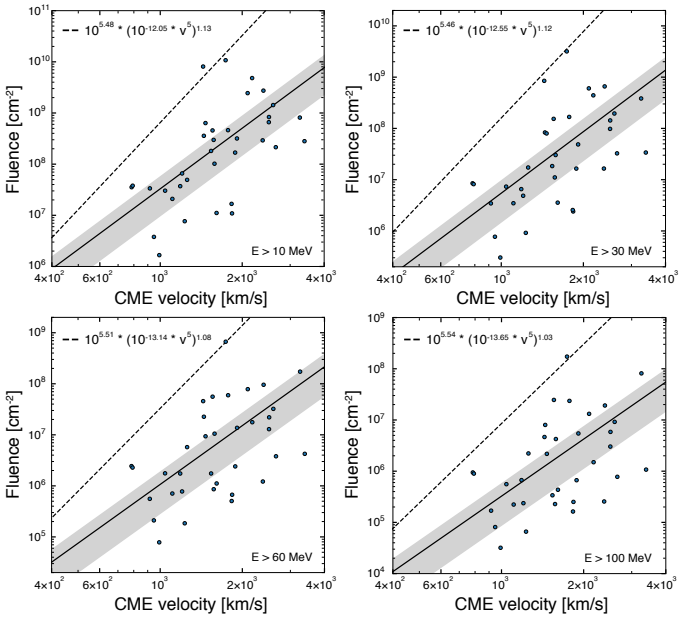

Fig. B.1. Relation between SEP fluence (F_P) and CME speed (V_{CME}) for the four integral energy bands of the SEP events, i.e., E>10-; E>30-; E>60-; and E>100 MeV, respectively. The log-log relations are obtained with RMA regression fitting. The estimated upper limits of F_P in terms of V_{CME} are depicted as dashed black lines in each panel.

Table B.1. *Upper limit* Peak Proton Fluxes (I_P, [pfu]) and Fluences (F_P, [cm^{-2}]) for the SEP event on AD774/775 and GLE05 derived in this work, for each integral proton energy. Peak proton fluxes were calculated via the $I_P \propto V_{CME}^5$ relations (provided in Figs. 1 & A.1) and Fluence via Equation 7 for a given $V_{CME,upper}$. The upper and lower limits included in the Table are driven by the V_{CME} range of the associated solar flare per event. The second and third columns provide outputs based on $V_{CME,upper}$ from Eq. (1), and the fourth and fifth columns provide the same results based on $V_{CME,upper}$ from Eq. (6) and the sixth and seventh columns provide the same results based on V_{CME} from Eq. (5).

	$V_{CME,upper}$ **| Eq.(1)**		$V_{CME,upper}$ **| Eq.(6)**		V_{CME} **| Eq.(5)**	
	AD774/775	**GLE05**	**AD774/775**	**GLE05**	**AD774/775**	**GLE05**
Integral Energy (MeV)	**Peak Proton Flux - I_P (pfu)**		**Peak Proton Flux - I_P (pfu)**		**Peak Proton Flux - I_P (pfu)**	
E>10	$2.26E{+}07^{3.17E+07}_{1.27E+07}$	$2.47E{+}06^{3.46E+06}_{1.39E+06}$	$6.16E{+}06^{7.92E+06}_{4.01E+06}$	$1.18E{+}06^{1.52E+06}_{7.71E+05}$	$6.23E{+}05^{8.58E+05}_{3.60E+05}$	$7.63E{+}04^{1.05E+05}_{4.41E+04}$
E>30	$7.16E{+}06^{1.00E+07}_{4.02E+06}$	$7.80E{+}05^{1.09E+06}_{4.38E+05}$	$1.95E{+}06^{2.50E+06}_{1.27E+06}$	$3.75E{+}05^{4.82E+05}_{2.44E+05}$	$1.97E{+}05^{2.71E+05}_{1.14E+05}$	$2.41E{+}04^{3.32E+04}_{1.40E+04}$
E>60	$1.84E{+}06^{2.58E+06}_{1.03E+06}$	$2.01E{+}05^{2.81E+05}_{1.13E+05}$	$5.01E{+}05^{6.44E+05}_{3.26E+05}$	$9.63E{+}04^{1.24E+05}_{6.27E+04}$	$5.06E{+}04^{6.98E+04}_{2.93E+04}$	$6.20E{+}03^{8.54E+03}_{3.59E+03}$
E>100	$5.69E{+}05^{7.97E+05}_{3.19E+05}$	$6.20E{+}04^{8.69E+04}_{3.48E+04}$	$1.55E{+}05^{1.99E+05}_{1.01E+05}$	$2.98E{+}04^{3.83E+04}_{1.94E+04}$	$1.57E{+}04^{2.16E+04}_{9.05E+03}$	$1.92E{+}03^{2.64E+03}_{1.11E+03}$
Integral Energy (MeV)	**Fluence - F_P (cm^{-2})**		**Fluence - F_P (cm^{-2})**		**Fluence - F_P (cm^{-2})**	
E>10	$6.18E{+}13^{9.05E+13}_{3.22E+13}$	$5.05E{+}12^{7.40E+12}_{2.63E+12}$	$1.42E{+}13^{1.89E+13}_{8.73E+12}$	$2.20E{+}12^{2.93E+12}_{1.36E+12}$	$1.07E{+}12^{1.53E+12}_{5.74E+11}$	$9.93E{+}10^{1.43E+11}_{5.35E+10}$
E>30	$1.37E{+}13^{2.00E+13}_{7.18E+12}$	$1.15E{+}12^{1.67E+12}_{6.00E+11}$	$3.19E{+}12^{4.23E+12}_{1.97E+12}$	$5.04E{+}11^{6.68E+11}_{3.11E+11}$	$2.45E{+}11^{3.51E+11}_{1.33E+11}$	$2.34E{+}10^{3.34E+10}_{1.26E+10}$
E>60	$1.89E{+}12^{2.72E+12}_{1.01E+12}$	$1.72E{+}11^{2.48E+11}_{9.24E+10}$	$4.63E{+}11^{6.07E+11}_{2.91E+11}$	$7.80E{+}10^{1.02E+11}_{4.91E+10}$	$3.90E{+}10^{5.51E+10}_{2.16E+10}$	$4.03E{+}09^{5.70E+09}_{2.23E+09}$
E>100	$2.93E{+}11^{4.15E+11}_{1.62E+11}$	$2.99E{+}10^{4.24E+10}_{1.65E+10}$	$7.68E{+}10^{9.95E+10}_{4.93E+10}$	$1.41E{+}10^{1.82E+10}_{9.03E+09}$	$7.25E{+}09^{1.01E+10}_{4.13E+09}$	$8.83E{+}08^{1.16E+09}_{4.74E+08}$

Appendix C: F_P-V_{CME} relations for E > 60 MeV and E > 100 MeV.

$$F_{\text{E>30 MeV}} = 10^{5.46} \cdot \left(10^{-12.55} \cdot V_{\text{CME}}^5\right)^{1.12} \quad \text{(C.1)}$$

$$= 2.53513 \cdot 10^{-9} \cdot V_{\text{CME}}^{5.6}$$

$$V_{\text{CME (E>30 MeV)}} = 34.2768 \cdot F_{\text{E>30 MeV}}^{0.178571} \quad \text{(C.2)}$$

$$F_{\text{E>60 MeV}} = 10^{5.51} \cdot \left(10^{-13.14} \cdot V_{\text{CME}}^5\right)^{1.08} \quad \text{(C.3)}$$

$$= 2.08353 \cdot 10^{-9} \cdot V_{\text{CME}}^{5.4}$$

$$V_{\text{CME (E>60 MeV)}} = 40.5163 \cdot F_{\text{E>60 MeV}}^{0.185185} \quad \text{(C.4)}$$

$$F_{\text{E>100 MeV}} = 10^{5.54} \cdot \left(10^{-13.65} \cdot v^5\right)^{1.03} \quad \text{(C.5)}$$

$$= 3.0234 \cdot 10^{-9} \cdot v^{5.15}$$

$$V_{\text{CME (E>100 MeV)}} = 45.11 \cdot F_{\text{E>100 MeV}}^{0.194175} \quad \text{(C.6)}$$

	F(E>30MeV)* [cm^{-2}]	v(E>30MeV)** [km/s]	F(E>60MeV)* [cm^{-2}]	v(E>60MeV)** [km/s]	F(E>100MeV)* [cm^{-2}]	v(E>100MeV)** [km/s]
	$1.57{\cdot}10^{11}$	3422	$4.90{\cdot}10^{10}$	3866	$2.04{\cdot}10^{10}$	4530
994 CE	$1.16{\cdot}10^{11}$	3242	$3.90{\cdot}10^{10}$	3706	$1.72{\cdot}10^{10}$	4383
	$6.30{\cdot}10^{10}$	2907	$3.20{\cdot}10^{10}$	3573	$1.42{\cdot}10^{10}$	4223
	$3.10{\cdot}10^{11}$	3864	$1.12{\cdot}10^{11}$	4506	$4.76{\cdot}10^{10}$	5341
775 CE	$2.42{\cdot}10^{11}$	3697	$9.40{\cdot}10^{10}$	4362	$4.13{\cdot}10^{10}$	5195
	$1.73{\cdot}10^{11}$	3482	$7.50{\cdot}10^{10}$	4183	$3.52{\cdot}10^{10}$	5037
	$4.06{\cdot}10^{11}$	4054	$1.36{\cdot}10^{11}$	4671	$5.45{\cdot}10^{10}$	5483
660 BCE	$2.41{\cdot}10^{11}$	3694	$9.90{\cdot}10^{10}$	4404	$4.38{\cdot}10^{10}$	5255
	$1.34{\cdot}10^{11}$	3326	$6.80{\cdot}10^{10}$	4108	$3.41{\cdot}10^{10}$	5006
	$2.12{\cdot}10^{11}$	3610	$9.50{\cdot}10^{10}$	4371	$4.89{\cdot}10^{10}$	5369
7176 BCE	$1.62{\cdot}10^{11}$	3441	$7.80{\cdot}10^{10}$	4214	$4.01{\cdot}10^{10}$	5166
	$9.00{\cdot}10^{10}$	3098	$4.30{\cdot}10^{10}$	3774	$2.37{\cdot}10^{10}$	4664

Table C.1. Column 1 gives the extreme SEP events. Columns 2, 4 & 6 provide the integral fluence F_P values for E> 30 MeV, E>60 MeV and E>100 MeV taken from Koldobskiy et al. (2023). Those correspond to a mean value with an upper and lower limit per event. These columns are marked with an (*). **Columns 3, 5 & 7 represented the derived V_{CME} directly obtained from Eqs. C.2, C.4, and C.6, per integral energy, respectively. The range of values considering all the integral fluence values F_P are: lower limit range: 2907 km/s - 5037 km/s, mean range: 3242 km/s - 5255 km/s; upper limit range: 3422 km/s - 5483 km/s.**

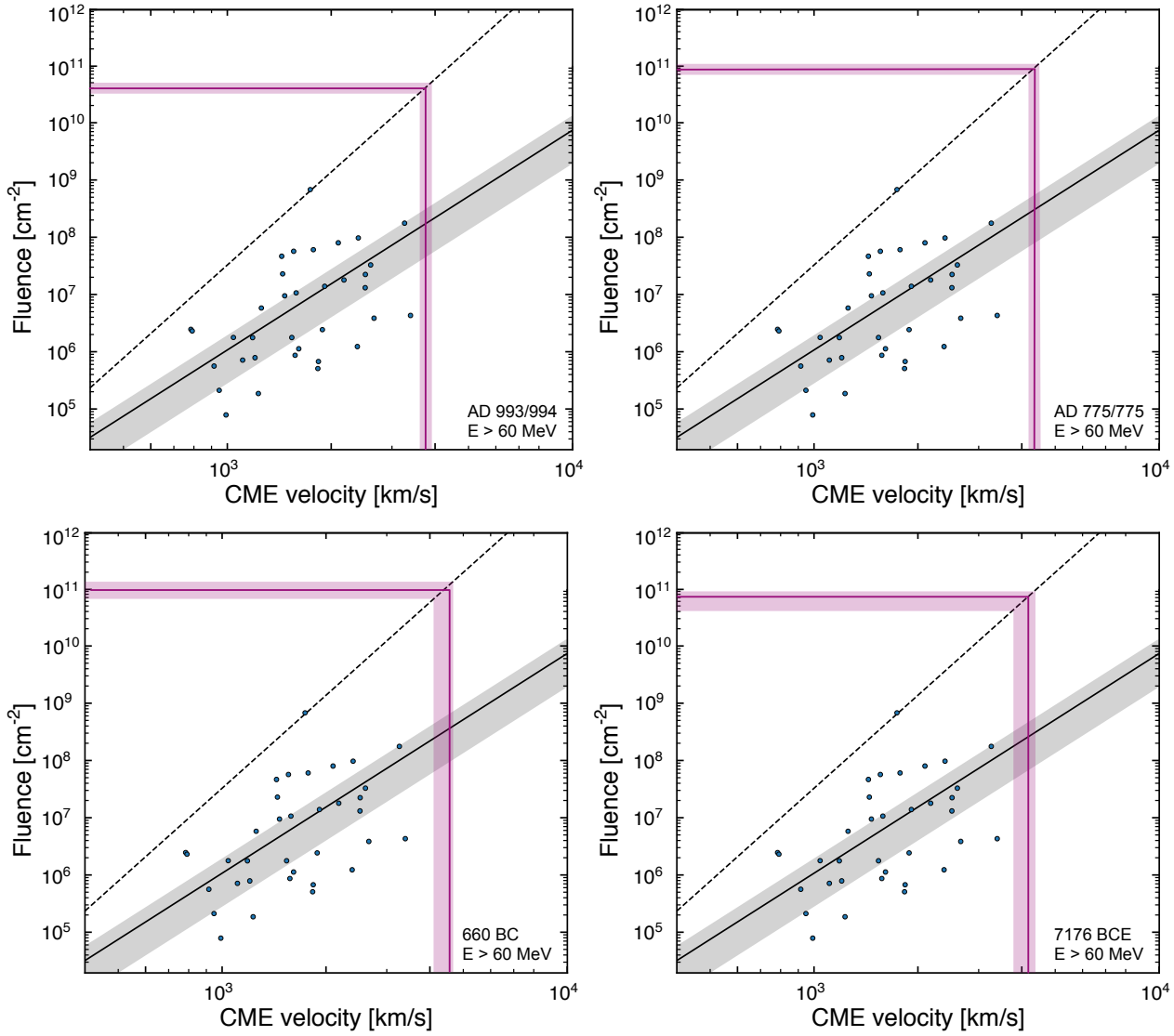

Fig. C.1. The same as Fig. 4 but for E>60 MeV.

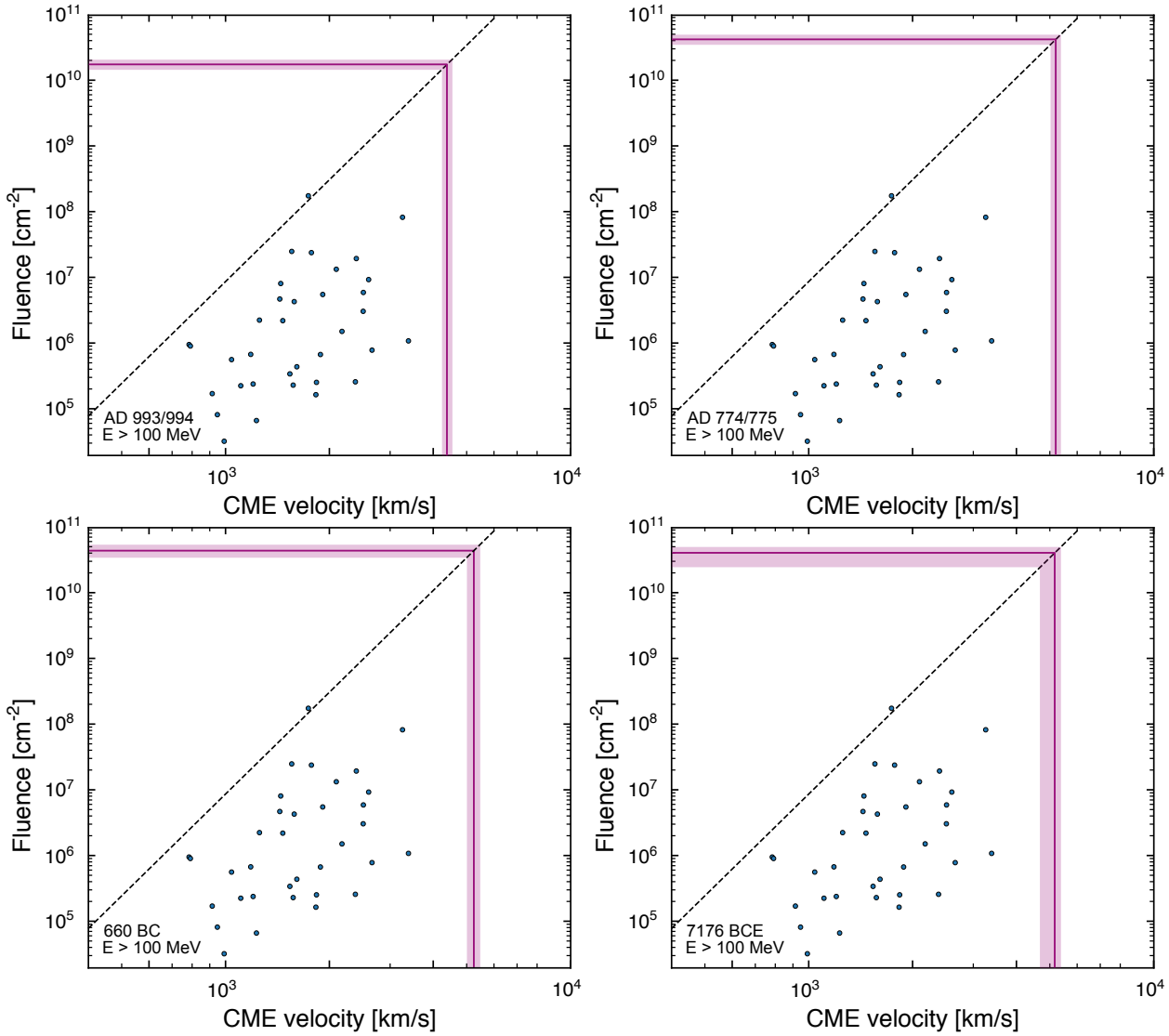

Fig. C.2. The same as Figs. 4 & C.1 but for E>100 MeV.